Journal of Alloys and Compounds, 195 (1993) 707–710
JALCOM 7563

Materials aspects of integrated high Tc dc-SQUID magnetometer fabrication

J.W.M. Hilgenkamp, R.P.J. IJsselsteijn, A.J.H.M. Rijnders, P.A.C. Tavares, J. Flokstra and H. Rogalla.

University of Twente, Department of Applied Physics, Low Temperature Division,
P.O. Box 217, 7500 AE Enschede, Netherlands.

Abstract

An integrated high Tc dc-SQUID magnetometer is being developed. It has in total 10 layers of five different materials. Various materials aspects of the fabrication process will be discussed, especially the smoothness of the films and the techniques to obtain smooth edges. Cross-overs and superconducting window contacts were fabricated. The critical temperature of the window-contact is 84K (j_c(77K)=$2 \cdot 10^5$ A/cm^2) and the resistivity of the insulating $SrTiO_3$ layer in the cross-over is $6 \cdot 10^5$ Ωcm at 77K. The complete coil often shows a small resistive component down to about 50K. Ramp type and bi-epitaxial grain boundary dc-SQUIDs show voltage modulation up to 65K and 79K, respectively. Efforts to fabricate an integrated high T_c dc-SQUID magnetometer will be discussed.

1. Introduction

To increase the field sensitivity of a dc-SQUID use is made of a flux transformer configuration. The flux transformer can be placed on a separate chip [1] or integrated on the same chip as the SQUID [2,3]. Since the integrated device consists of a large number of layers good control of layer growth is a prerequisite. Occurrence of outgrowths and holes in the films has to be minimized. Care has to be taken to avoid interface reactions. To provide high quality epitaxial growth of the layers over structures etched in underlying layers, these structures should have smooth edges [4]. Irregular or steep edges may leed to unwanted grain boundaries and even short cuts. Ar ion beam etching under an angle provides these smooth edges. Separate cross-overs, window contacts and multiturn coils have been fabricated to test this etching procedure.

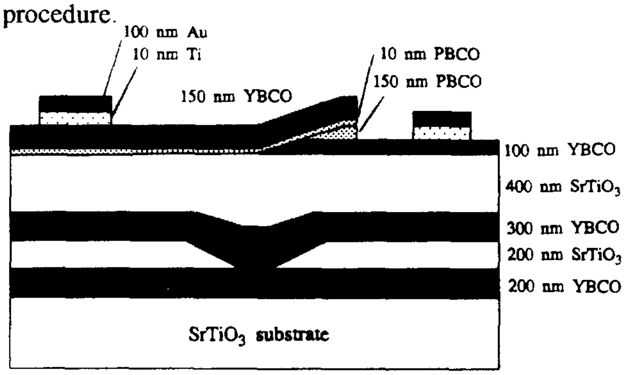

Figure 1: Schematic cross section of the integrated magnetometer.

The key elements of the dc-SQUIDs are the Josephson junctions. Besides good performance (high IcRn-products at high temperatures, low noise levels, stability and reproducibility) they have to be compatible with the techniques used for fabrication of the total device. In our group $YBa_2Cu_3O_{7-x}$ (YBCO) / $PrBa_2Cu_3O_{7-x}$ (PBCO) / YBCO ramp type junctions and bi-epitaxial grain boundary junctions with various weak link angles are presently investigated.

2. Design

In figure 1 the design of the integrated dc-SQUID magnetometer is schematically shown.

The coil structure is placed directly on the substrate beneath the SQUID-washer. In this way the fabrication of the junctions is the last step in the process. The coil windings and the returnstrip are separated by a $SrTiO_3$ layer. A window provides a superconducting contact between these layers in the centre of the coil. After structuring the returnstrip of the coil a 400 nm thick $SrTiO_3$ insulation layer is deposited to separate the coil from the SQUID washer.

The YBCO/PBCO bi-layer that serves as the base electrode of our junctions is deposited in situ. After definition of the junction ramp by photolithography and Ar-ion beam etching under an angle, the ramp is cleaned by Ar ion milling before in situ deposition of the barrier and top layers takes place. In the case when bi-epitaxial grain boundary

0925-8388/93/$06.00

junctions are used an MgO/CeO_2 bi-layer is deposited in situ after the $SrTiO_3$ insulation layer has been deposited. After structuring the CeO_2 template layer and cleaning of the edge by Ar ion milling the YBCO junction layer is deposited in situ.

A contact layer of Ti and Au is then deposited by RF magnetron sputtering and structured by lift off before, as a final step, the square washer dc-SQUID structures are defined by Ar ion-beam or Ar plasma etching.

The 5 turn input coil has 8 μm wide windings, separated 5 μm from each other. It is connected to a 3.1 x 4 mm^2 pick up coil or to contact pads. In the latter case the $SrTiO_3$ is removed from the contacts by selective etching with a 2% HF solution in H_2O [5] followed by a short Ar plasma cleaning treatment.

The washer has an outer dimension of 150μm x 155μm and a hole size of 16μm x 16μm. The inductance L is estimated to be about 30pH. The slit inductance is partly shielded by placing it over the return strip of the input coil. The junctions have a width of 12μm. In the case of the ramp type junctions the critical current can be set to 32 μA at the working temperature by adjusting the barrier thickness so that the screening factor $\beta_L(=2LI_c/\phi_o)$equals 1.

3. Deposition

RF magnetron sputtering [6] is used for the junction barrier and top layer as well as the contact layers, and pulsed laser deposition [7] for the other layers. We use $SrTiO_3$ substrates. Yttrium stabilized ZrO_2 (YSZ) substrates were not applicable, because after structuring the coil windings subsequent deposition of $SrTiO_3$ resulted in 80% (110) orientation, inducing mainly (103) oriented YBCO in the return strip. This problem does not occur if $SrTiO_3$ substrates are used.

We have studied the influence of the process parameters of laser deposition on the occurrence of droplets and outgrowths in YBCO films [8]. The droplet density is minimal when a laser fluence below about 1.0 J/cm^2 is used. The outgrowth density decreases with increasing laser pulse rate or decreasing deposition temperature. High quality smooth films, with an outgrowth density below 1 per $100\mu m^2$, were obtained at a rate of 10 Hz and a deposition temperature of 720°C. The oxygen pressure is 25 Pa. Large differences in the smoothness of $YBCO/SrTiO_3$ bi-layers caused by only small changes in deposition temperature were observed. The difference of the deposition temperatures for a closed smooth surface and for a surface with holes or outgrowths is only 10°C. We found an optimal deposition temperature of 730°C with an oxygen pressure of 15 Pa and a laser pulse energy of 1.4 J/cm^2. Sputtered YBCO films are deposited at 740°C with a sputter pressure of 13Pa. The Ar/oxygen ratio is 3:2.

The deposition conditions for YBCO and PBCO are similar.

The optimal deposition parameters were derived from single, bi- or tri-layer studies. The influence of a larger number of underlying layer on the optimal deposition parameters is studied.

4. Etching

To provide epitaxial growth, structures should have edges that are very smooth with an angle of 30° or less with the substrate surface. Wet chemical methods do not yield these smooth edges and also Ar plasma etching is not suitable.

We use Ar ion beam etching under an angle to obtain low angle edges in our structures. An AZ 1518 photoresist layer is baked out in an oven at 90°C for 10 minutes. The energy of the incident ions is 500eV. The beam current is 10mA and the angle used is 45°. The structuring is performed intermittently at an Ar pressure of $5 \cdot 10^{-2}$Pa resulting in an effective etch-rate of 38 nm/min for YBCO and 23 nm/min for $SrTiO_3$. In one run both edges of a stripline can be etched in the correct way [8].

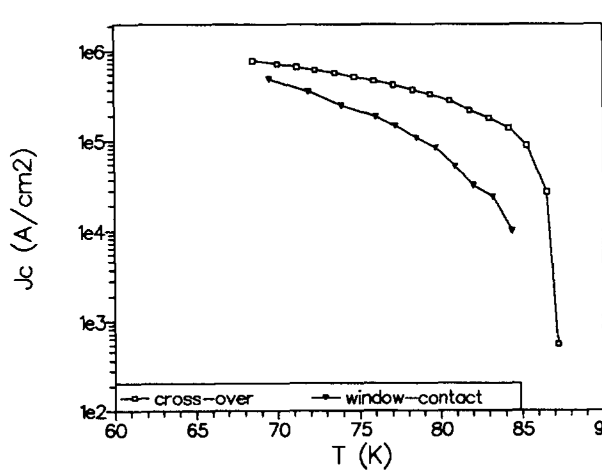

Figure 2: J_c as a function of T for the window contact and the top-strip of the cross-over.

Using the Ar ion gun etching procedure separate cross-overs, window contacts and multiturn coils have been fabricated. In figure 2 the critical current density of a window contact and the top-strip of a cross-over is shown as a function of T.

The base YBCO layer of the cross-over has a thickness of 200 nm and is etched into a stripline of 150 μm width using the ion beam method. On top of this a 150 nm (100) oriented $SrTiO_3$ layer is grown. The 200 nm thick YBCO top layer is structured into a 30μm wide stripline using Ar ion plasma etching. The critical temperature of the top layer is 87K. j_c at 77K equals $5{\cdot}10^5$ A/cm^2. The resistivity of the $SrTiO_3$ layer at 77K is $6{\cdot}10^5$ Ωcm. Window contacts were fabricated with a critical temperature of 84K and a critical current density of $2{\cdot}10^5$ A/cm^2 at 77K. The contact has an effective area in the ab-plane of 2.5 μm^2.

The quality of the small number of coils that we have made so far is not as good as that of the separate cross-overs and windows. The best coil had a T_c of 50K. It is a 12.5 turn coil with a linewidth of 30μm. The total length is 4.6 cm. The window-contact is 30 μm x 60 μm. We believe that the problem occurs in the return strip of the coil.

5. Junctions and DC-SQUIDs

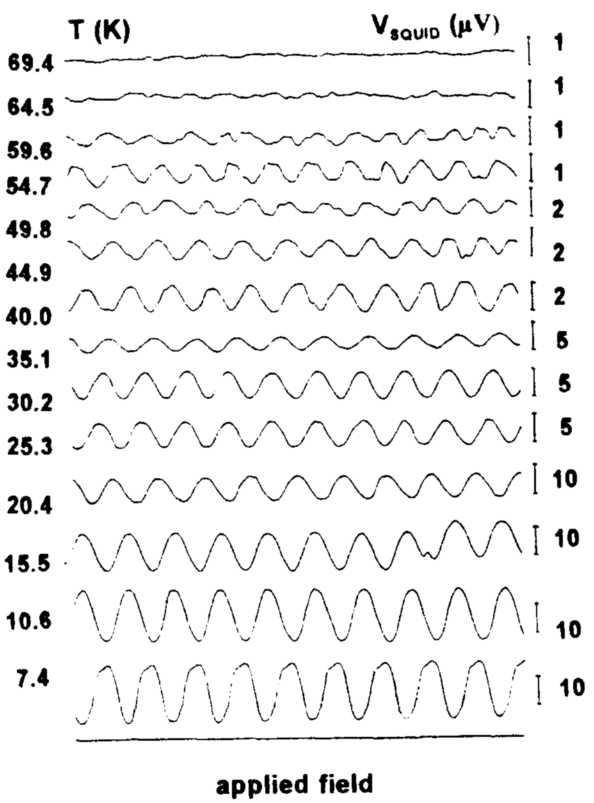

Figure 3: V(ϕ) as a function of temperature for a ramp type DC-SQUID.

YBCO/PBCO/YBCO ramp type junction [9] and bi-epitaxial grain boundary junctions with weak link angles of 18° and 27° [10] are presently studied in our group. The ramp type junctions are characterized by rather high I_cR_n products, up to 8mV at 4.2K. By varying the barrier thickness the critical current of the junctions can more or less be adjusted. I_c and R_n have been measured as a function of temperature and Shapiro steps have been observed up to 80 K [11].

DC-SQUIDs based on ramp type junctions showed voltage modulation up to about 65 K. The voltage modulation by an applied magnetic field is shown at various temperatures in figure 3. Nicely periodic behaviour was observed over several thousands of flux quanta.

The noise power spectrum of one of our SQUIDS was measured at 4.2K. The self-inductance of this sample was about 100 pH. The critical current was 20 μA, $\beta_L = 2$. The white noise level at frequencies above 40 Hz was 10^{-27}J/Hz. Below 40 Hz the noise predominantly has a 1/f character resulting in a noise level of $8{\cdot}10^{-27}$J/Hz at 1Hz. It is not clear however if these high noise levels are structural for these types of junctions or that this is specific for this sample.

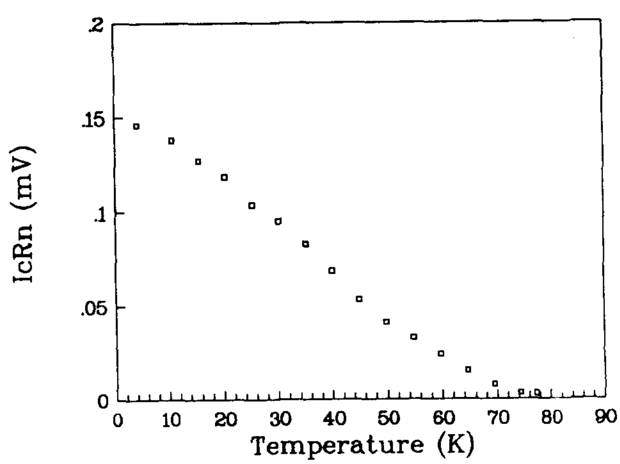

Figure 4: I_cR_n product as a function of temperature for an 18° bi-epitaxial grain boundary SQUID.

Bi-epitaxial grain boundary junctions and dc-SQUIDs with weak link angles of 18° and 27° have been fabricated. The maximum operation temperature for these devices is about 80 K. The temperature dependence of the I_cR_n product for an 18° dc-SQUID is given in figure 4. The junctions have a width of 10 μm and a thickness of 200 nm. The R_n value is about 1Ω independent of temperature. The voltage modulation of this SQUID is shown in figure 5 for different values of the bias current at 77K. The maximum modulation depth at this temperature is 1.5µV.

The noise level at 4.2K was 10^{-28}J/Hz at 100Hz. Below this frequency the noise has a 1/f character.

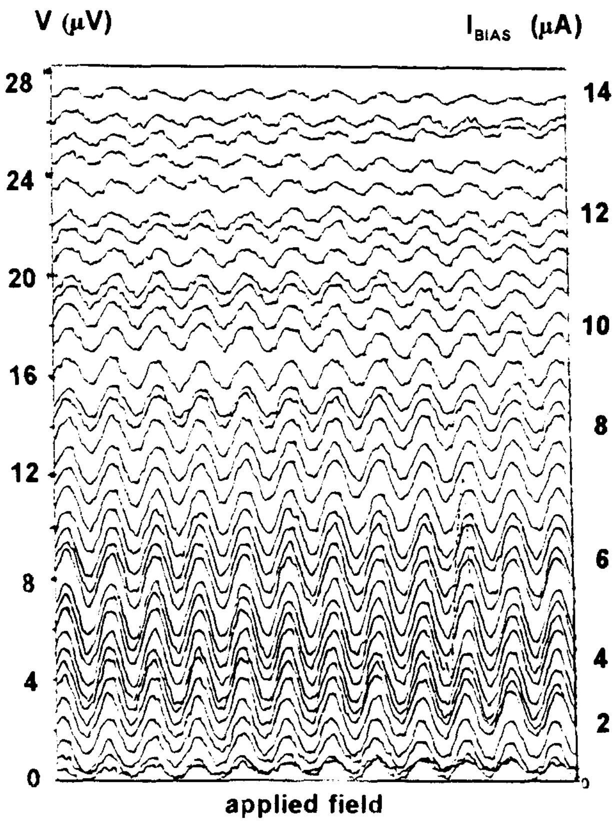

Figure 5: V(ϕ) for different values of the bias current for an 18° bi-epitaxial grain boundary SQUID at 77K.

The design was however not optimal at this temperature for β_L = 10. Considerable improvement of the noise levels may be expected by the use of a bias reversal method.

6. Integrated DC-SQUID magnetometer

Although the basic elements for an integrated dc-SQUID magnetometer could be prepared, a complete integration was not succesful for the first three trials up to now. The coil structure functioned as described but some influence of later processing steps was noticeable. The base electrode on top of the $SrTiO_3$ insulating layer is superconducting at 78 K but the ramp type junctions did not function adequately. The smoothness of the multilayer structure underneath is probably not good enough. Improvement may be expected when also the junction structures are realised on the substrate. Further work is in progress.

7. Conclusions

Several material aspects relevant for the fabrication of an integrated high T_c dc-SQUID magnetometer have been studied. Using optimal deposition parameters reasonable flat layers could be fabricated. Ar ion beam etching is a fruitfull technique for the fabrication of smooth edges necessary for cross-overs, window contacts and other ramps. High quality window contacts and cross-overs were made but coils often showed a resistive tail down to 50K. Ramp type and bi-epitaxial dc-SQUIDs were fabricated with operation temperatures up to 80 K. The complete integration of all elements to an integrated dc-SQUID magnetometer failed up to now.

References

[1]: F.C. Wellstood, A.H. Miklich, J.J. Kingston, M.J. Ferrari, J. Clarke, M.S. Colclough, K. Char and G. Zaharchuk, *SQUID'91* Berlin p. 162

[2]: A.H. Miklich, D. Koelle, E. Dantsker, D.T. Nemeth, J.J. Kingston, R.F. Kromann and J. Clarke, ASC'92, Chicago.

[3]: L.P. Lee, K. Char, M.S. Colclough and G. Zaharchuk, Appl. Phys. Lett. 59, 3051, (1991).

[4]: C.L. Jia, B. Kabius, K. Urban, K. Herrman, G.J. Cui, J.S. Schubert, W. Zandler, A.I. Braginski and C. Heiden, Physica C 171, 545, (1991).

[5]: W. Eidelloth, W.J. Gallagher, R.P. Robertazzi, R.H. Koch, B. Oh, R.L. Sandstrom, Appl. Phys. Lett 59, 1257, (1991).

[6]: J. Gao, B. Häuser and H. Rogalla, J. Appl. Phys. 67, 2512, (1990).

[7]: D.H.A. Blank, D.J. Adelerhof, J. Flokstra and H. Rogalla, Physica C 167, 423, (1990).

[8]: J. Flokstra, R.P.J. IJsselsteijn and J.W.M. Hilgenkamp, Thin Solid Films, 218, 304, (1992).

[9]: Yu. Boguslavskij, J. Gao, A.J.H.M. Rijnders, D. Terpstra, G.J. Gerritsma and H. Rogalla, Physica C, 194, 268, (1992).

[10]: R.P.J.IJsselsteijn, J.W.M. Hilgenkamp, M. Eisenberg, C. Vittoz, J. Flokstra and H. Rogalla. E-MRS, Strasbourg, fall 1992.

[11]: D. Terpstra, Private Communications.